University of Huddersfield Repository

Payne, B.S., Gu, Fengshou, Webber, C J S and Ball, Andrew

Componential coding in the condition monitoring of electrical machines Part 2: application to a conventional machine and a novel machine

Original Citation

Payne, B.S., Gu, Fengshou, Webber, C J S and Ball, Andrew (2003) Componential coding in the condition monitoring of electrical machines Part 2: application to a conventional machine and a novel machine. Proceedings of the Institute of Mechanical Engineering Part C, Journal of Mechanical Engineering Science, 217 (8). pp. 901-915. ISSN 0954-4062

This version is available at http://eprints.hud.ac.uk/id/eprint/6810/

The University Repository is a digital collection of the research output of the University, available on Open Access. Copyright and Moral Rights for the items on this site are retained by the individual author and/or other copyright owners. Users may access full items free of charge; copies of full text items generally can be reproduced, displayed or performed and given to third parties in any format or medium for personal research or study, educational or not-for-profit purposes without prior permission or charge, provided:

- The authors, title and full bibliographic details is credited in any copy;
- A hyperlink and/or URL is included for the original metadata page; and
- The content is not changed in any way.

For more information, including our policy and submission procedure, please contact the Repository Team at: E.mailbox@hud.ac.uk.

http://eprints.hud.ac.uk/

Componential coding in the condition monitoring of electrical machines
Part 2: application to a conventional machine and a novel machine

B S Payne[1], **F Gu**[1], **C J S Webber**[2] and **A D Ball**[1]*
[1]Maintenance Engineering Research Group, Manchester School of Engineering, University of Manchester, UK
[2]QinetiQ, Malvern, UK

Abstract: This paper (Part 2) presents the practical application of componential coding, the principles of which were described in the accompanying Part 1 paper. Four major issues are addressed, including optimization of the neural network, assessment of the anomaly detection results, development of diagnostic approaches (based on the reconstruction error) and also benchmarking of componential coding with other techniques (including waveform measures, Fourier-based signal reconstruction and principal component analysis). This is achieved by applying componential coding to the data monitored from both a conventional induction motor and from a novel transverse flux motor. The results reveal that machine condition monitoring using componential coding is not only capable of detecting and then diagnosing anomalies but it also outperforms other conventional techniques in that it is able to separate very small and localized anomalies.

Keywords: neural network, componential coding, auto-encoder, condition monitoring, induction motor, transverse flux motor, fault detection, fault diagnosis

NOTATION

ADI	average discrimination index
ICAN	Independent Channel Architecture Network
IR	inner root (of transverse flux motor stator core)
IT	inner tip (of transverse flux motor stator core)
JCAN	Joint Channel Architecture Network
OR	outer root (of transverse flux motor stator core)
OT	outer tip (of transverse flux motor stator core)
VDI	variance discrimination index

The MS was received on 19 November 2002 and was accepted after revision for publication on 22 May 2003.
* *Corresponding author: Maintenance Engineering Research Group, Manchester School of Engineering, University of Manchester, Oxford Road, Manchester M13 9PL, UK.*

1 INTRODUCTION

Electric motors are at the core of most engineering processes. In general they are inherently reliable (because of their mechanical simplicity) and require very little attention, except at infrequent intervals when the plant is shut down for inspection. Nevertheless, like any electromechanical system, electric motors do fail. Unanticipated failure can lead to very costly downtime and consequential damage [**1**, **2**]. Hence early and accurate fault detection and diagnosis through condition monitoring is of key importance. Within the last decade, much effort has been placed on research and development in this field.

The interpretation of vibration and per-phase current data is by far the most widely developed means of determining incipient motor faults. In particular, casing vibration monitoring is well established and is capable of detecting a wide range of mechanical motor problems (such as shaft eccentricity/misalignment [**1**, **3**, **4**], bearing faults [**1**, **5**], looseness [**5**, **6**] and rotor imbalance [**7**]) in addition to broken rotor bars (which, strictly speaking, are considered as an electrical fault) [**1**, **2**, **8**, **9**]. Per-phase current measurement and analysis is an approach

that has more recently been capitalized for motor monitoring. Several researchers and industrial practitioners have used per-phase current to detect and diagnose eccentricity [**3**, **10**], broken rotor bars [**11–13**], phase imbalance [**14**] and bearing problems [**15**, **16**].

Analysis of airborne acoustic data is a particularly new method that has been investigated to detect and diagnose loose stator coils [**17**], phase imbalance [**14**], misalignment [**14**], broken rotor bars [**14**] and bearing faults [**18**]. The references detail that in some cases acoustic monitoring has the potential to outperform vibration-based approaches in the early detection of incipient faults. In addition, transducer set-up is easier for acoustic monitoring than for vibration monitoring, and transducers (microphones) are also non-contacting and thus reduce concerns related to overheating and attachment [**14**].

Another method used for motor condition monitoring is flux measurement. Flux in the air gap between the rotor and stator is directly related to the operational characteristics of an electric machine and hence is likely to produce accurate indications of electrically related fault conditions. Albright [**19**] placed search coils to measure changes in the air gap flux and hence to detect broken rotor bars. A discussion is also made by Tavner and Penman [**2**] and Penman *et al.* [**20**] on the possibilities of using axial flux measurement to detect conditions such as eccentricity and phase imbalance. However, from a practical perspective these approaches can be difficult to implement [**21**] and, therefore, have not widely been applied.

Clearly a range of measurement parameters exists for the condition monitoring of electrical machines. However, measurement of data alone does not fulfil condition monitoring objectives; the crux of condition monitoring is the extraction of useful condition-indicating information from the measured data.

Spectral analysis of data signal frequency components is one of the most commonly used methods for interpretation of the health of a machine [**22**]. Frequency spectra can be obtained from hand-held data collectors, dedicated signal analysers or ready-written routines in software packages such as MATLAB®. Interpretation of many spectral features (such as fundamental frequencies, sidebands and harmonics) can be relatively straightforward, permitting close correlation with physical machine characteristics.

With the rapid increase in computational capability that has been experienced in the last decade, more advanced data processing techniques have become viable in the application to machinery condition monitoring. As cited in section 1 of Part 1 of this paper [**23**], these include time–frequency analysis, timescale analysis, higher-order statistical analysis and independent component analysis.

Artificial neural networks have also been widely studied for fault detection and diagnosis purposes. They are often applied as a post-processing tool, with the input variables having been extracted by more conventional signal processing techniques. For example, Chow and Yee [**24**] present several applications of neural networks to incipient fault detection in rotating machines (including induction motors) by using parameters derived from per-phase power supply current as input variables. Filippetti [**25**] proposed a method that adopts both induction motor slip and phase current as the network input variables. Paya *et al.* [**26**] describe a method for detecting motor bearing faults using vibration data that have been pre-processed by a wavelet transformation. Clearly, the performance of the network depends on the choice of input variables and making the appropriate selection can be a less-than-straightforward task. A potential solution to this problem is to apply neural networks directly to raw data, thus making better use of the non-linearity benefits of neural modelling [**27**].

In general, even given the advances that have been made, the majority of current monitoring techniques and software often give inaccurate results and are also poor at:

1. Handling data collected simultaneously from several channels, because most extract fault features on a channel-by-channel basis. This is a disadvantage because most machines give a change in multiple measurement channels when a fault occurs and correlations between these channels can provide crucial detection and diagnosis information.
2. Monitoring novel machines. The reason for this is that a highly beneficial aid in condition monitoring is prior knowledge, as previous experience often plays an important role in fault detection and diagnosis. By definition, for the condition monitoring of a novel motor, this prior knowledge does not exist.

As explained in Part 1 [**23**], componential coding models data in an adaptive way and derives signal features automatically using a computationally efficient algorithm. It therefore has the potential to perform accurate fault detection and is applicable to monitoring novel machines. In addition, componential coding also enables simultaneous analysis of multiple data channels.

To investigate the capabilities of componential coding in fault detection and diagnosis, two lines of investigation were followed. Firstly, an application to noise-contaminated vibration and airborne acoustic data from a conventional induction motor was made. This enabled the use of componential coding in the condition monitoring of a familiar machine, for which conventional means of monitoring are well understood, which hence aided the interpretation of the results. Secondly, componential coding was applied to multichannel magnetic flux data from a novel electric motor. This provided an opportunity to investigate the application

of componential coding to a previously unseen machine, and for which limited failure mode information was available.

2 APPLICATION TO A CONVENTIONAL INDUCTION MOTOR

2.1 Introduction

Componential coding was first applied to data recorded from a 3 kW, three-phase, direct-on-line induction motor. Induction machines are the single most common industrial prime movers and because they often operate in critical applications, this increases the need for effective condition monitoring. It is well known that stator asymmetry faults are of particular concern [**28**–**30**] and, therefore, a motor test facility was used to seed voltage imbalance faults in one phase of the power supply [**14**]. Routine vibration data were recorded from the motor casing and acoustic measurements were also taken (as previous work has demonstrated, this has potential in this application [**14**, **17**, **31**]).

2.2 Seeding of power supply phase imbalance faults

Two main types of imbalance may be found in three-phase supplies: structural and functional. Structural imbalance occurs because, for economic reasons, the physical structure of transformers, and especially lines, is not balanced [**30**]. This leads to imbalanced voltages even if the generator voltages and load currents are perfectly balanced. The amount of structural imbalance may also be made worse by poor power management by the consumer. For example, the single-phase lighting in a large building may be powered unevenly from one phase or power demands may not have been considered appropriately in the extension of a building.

The second type of imbalance, functional imbalance, is due to fluctuations of consumer demand on the three-phase supply. Large machines, such as a large motor or an arc welder [**21**], are particular causes of this type of imbalance because of their high current requirements. Alternatively, a bad electrical contact (due to dirt, oxidation or a loose connection) will result in increased voltage drop across that contact and thus reduce the proportion of voltage across the motor windings. Current leakage to earth, caused, for example, by insulation breakdown, may also lead to phase imbalance.

Imbalance problems are also compounded by the use of three-phase variable-speed controllers, as some of the more common controllers on the market only have typical imbalance accuracies of 3 per cent (7.2 V in the 240 V UK supply). The motor test rig allowed for controlled imbalances of both 20 V (8.3 per cent) and 40 V (16.7 per cent) to be induced by dropping the voltage on one phase with a centre-tapped transformer.

Power supply imbalance to a motor results in additional losses and overheating—as a rule of thumb the winding temperature rises by 25 per cent for every 3.5 per cent voltage imbalance [**28**]. From the authors' experience, phase imbalance is thus sometimes the cause of apparently random overheating of electric machines in industry. Temperature rises cause thermal ageing and make the winding insulation, in particular, more vulnerable to electric, mechanical and environmental stresses [**28**]. Voltage imbalance is thus an important cause to consider in motor failure and there are clear benefits in detecting its occurrence from measured motor parameters.

2.3 Vibration and acoustic data-sets

Componential coding was applied to two channels of recorded data. Surface vibration was recorded in a routine and standard way using an accelerometer mounted close to the bearing on the drive-end end-cap (as this is a major vibration transmission path between the rotor and stator and, therefore, provides information on both machine parts). Airborne acoustics was recorded using a microphone pointed towards the motor and placed at 200 mm perpendicularly from the motor centre height. In contrast to routinely measured vibration data, it is unusual to measure acoustic data, although it is a technique that is receiving increasing interest.

Data were collected at 75 per cent of the rated motor load, under healthy operation (which will be referred to as case 0) and with the seeding of a 20 V imbalance fault (case 1) and a 40 V imbalance fault (case 2). The vibration and acoustic data were sampled simultaneously at 32.5 kHz, giving a usable bandwidth of 0–15 kHz. For each fault case, three data records were collected—each of 65 536 points and covering more than 30 shaft revolutions. This large data record size was used to ensure that componential coding was trained sufficiently and that a reliable model was obtained to represent the underlying data features. Figure 1 shows a portion of each data record and illustrates that no clear differences can be seen between the raw data for the different operational cases.

2.4 Componential coding configuration and optimization

Section 2.1 of Part 1 of the paper [**23**] describes how componential coding may be implemented through either of two network variants. In summary, the Joint Channel Architecture Network (JCAN) implementation

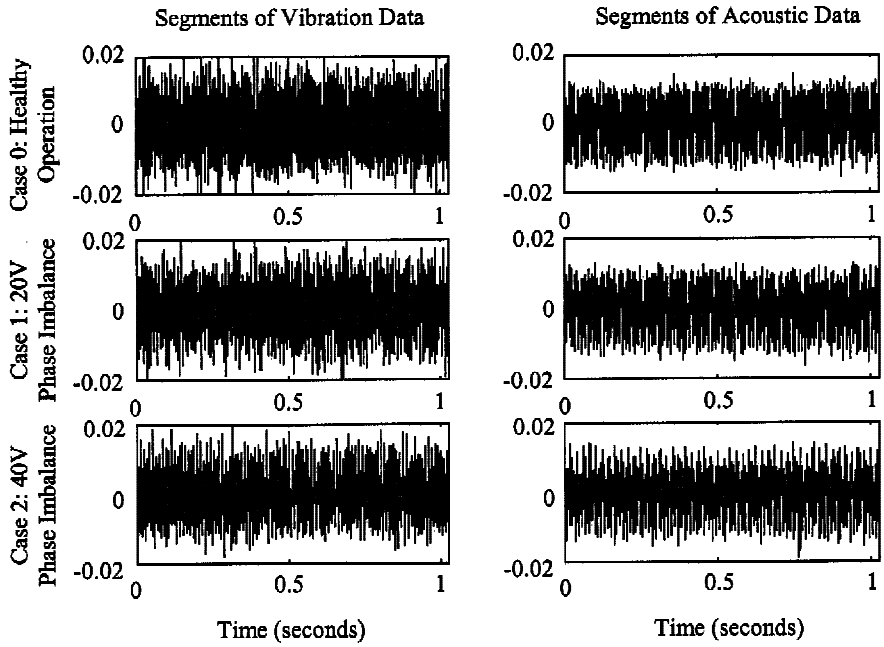

Fig. 1 Vibration and acoustic data (normalized amplitudes)

can detect anomalous* correlations (including phase relationships) between simultaneously applied data channels. Alternatively, the Individual Channel Architecture Network (ICAN) may be employed in order to model the characteristics of individual channels in order to de-emphasize interchannel correlations. Both the JCAN and the ICAN were studied for the separation of the two degrees of severity of voltage imbalance from the baseline condition.

Section 1.2 of Part 1 [**23**] discusses how componential coding modelling is achieved by deriving basis vectors through the adaptive training process. The dimension of the basis vectors (i.e. the number $n_s n_t$ of coordinates comprising a basis vector, using the notation of Part 1 [**23**]) is chosen to cover at least two periods of the observed principal frequency component in the monitored data. This is because at least one complete period is required to model any cyclic information. Within reason, the actual dimension of a basis vector is a compromise between computational speed and modelling accuracy. Previous work has found a basis vector dimension of 64 data points to be a good compromise for the induction motor data [**32**]. Signal resampling is necessary to ensure that each basis vector of dimension 64 points covers two periods of the principal frequency (which may be different for different data sources). For the vibration and acoustic data this was achieved by desampling by a factor of 2 and 10 respectively.

Componential coding also requires the setting of its two most influential non-adaptive parameters: threshold (which determines how many of the neurons activate) and the number of basis vectors. These parameters were optimized to maximize anomaly discrimination using an automated genetic algorithm. The final configurations for the two network variants, following optimization, are summarized in Table 1. The ICAN, with its inherent independent nature, has a separate configuration for each type of data, whereas the JCAN has one configuration for both vibration and acoustics.

The values given in the last two rows are average discrimination indices (ADIs) which, as explained in section 2.7 of Part 1 [**23**], indicate the difference in newly applied data-sets from baseline healthy motor operation data (from case 0). These rows show the difference between the model reconstruction and previously unseen healthy data (from case 0) and the difference between the model reconstruction and data recorded with the introduction of a 20 V imbalance fault (case 1) respectively.

As expected, the ADI values are close to zero when componential coding is applied to previously unseen healthy data from case 0 (section 2.7 of Part 1 [**23**]), because it is similar to the data on which the model was trained. However, when componential coding is applied to data recorded under faulty operation, the ADI values for each configuration are clearly much larger. This indicates that both the ICAN and JCAN are capable of separating the anomalous case 1 from the baseline

* As described in section 1.1 of Part 1 of this paper [**23**], an anomaly is any characteristic of an unseen data-set that is different from the characteristics of the training data-set. A fault can be thought of as a special case of an anomaly in which the anomalous characteristic happens to arise as the result of a real fault in the engineering system being monitored.

Table 1 Optimized componential coding configuration for induction motor data

Componential coding variant	ICAN		JCAN
Data-set	Vibration	Acoustics	Vibration and acoustics
Basis vector dimension	64	64	128 (i.e. 64 + 64)
Threshold value	0.101	0.854	0.113
Number of basis vectors	23	23	26
ADI (case 0)	0.006	0.009	0.056
ADI (case 1)	0.417	0.931	0.289

case 0. In addition, the higher ADI values for the two separate ICAN configurations show that this network produces better detection results than the JCAN in this context. This is particularly true for the acoustic data and, hence, reveals that componential coding is more sensitive to the seeded fault condition when applied to this form of data. This may be because experience has shown that a single channel of acoustic data often gives a more comprehensive picture of condition than a single channel of surface vibration [**33**].

It can also be seen in Table 1 that the optimized threshold for the ICAN is much higher for the acoustic data than that for the vibration data. The higher threshold for the acoustic data reflects the fact that there is more similarity between input patterns, so the threshold may be set so high that neurons only activate when basis vectors are very similar to the measured acoustic data. Conversely, there is less similarity between input patterns for the vibration data, so a small threshold is needed to achieve a small model residual with baseline control data. In this case, neurons will activate even if the match between a basis vector and the vibration data is less good. From an anomaly detection perspective, a higher threshold allows greater sensitivity to smaller changes between the baseline and monitored data.

2.5 Anomaly detection

So far this paper has shown the ability of both the ICAN and JCAN to detect seeded voltage imbalance faults on the basis of the ADI measure. An alternative measure is the variance discrimination index (VDI). As discussed in section 2.7 of Part 1 [**23**], the ADI is based on the averaged reconstruction errors over the monitored data-set and is, consequently, most useful when a relatively large proportion of the monitored data-set is anomalous. The VDI is based on the variance of the reconstruction errors and is, therefore, more capable of highlighting anomalies that manifest themselves only over a relatively small portion of data.

Table 2 shows that both the ADI and VDI increase with severity of fault condition. Therefore both the ICAN and the JCAN provide clear discrimination of fault severity.

Both the ICAN and the JCAN demonstrate good fault detection with both the ADI and VDI (although the ICAN provides better detection results in this context). Significantly, the acoustic ICAN outperforms the vibration ICAN. This latter observation suggests that the acoustic signal contains more (useful) global information related to the motor operation and the voltage imbalance problem. The acoustic signal is generated not only from the end-cap vibration measured but also from sources including the main casing body, the cooling fan and the mount base. Any changes of these sources, due to the introduction and increasing severity of the fault condition, would be incorporated in the acoustic signal. In contrast, the vibration is measured at a specific location that does not fully represent the change in the motor characteristics [**33**].

2.6 Anomaly diagnosis using the residual spectrum

Fault diagnosis of many induction motor failure modes is well understood using conventional frequency domain methods [**22**]. Componential coding can also diagnose faults through frequency domain approaches. Since the

Table 2 Discrimination index values with the introduction of phase imbalance

Componential coding variant	ICAN				JCAN	
Data-set	Vibration		Acoustics		Vibration and acoustics	
Discrimination index	ADI	VDI	ADI	VDI	ADI	VDI
Case 0 (healthy operation)	0.006	0.001	0.009	0.002	0.056	0.001
Case 1 (20 V phase imbalance)	0.417	0.847	0.931	2.037	0.289	1.091
Case 2 (40 V phase imbalance)	0.653	0.988	1.546	0.087	0.513	1.139

reconstruction errors represent the uniqueness of a new measurement, the spectrum of the residual signal correspondingly characterizes the changes in the frequency structure. (The residual signal, called the anomaly vector in Part 1 [**23**], is defined as the vector difference between the current input data vector and the network's model-based reconstruction of that input data vector.) Changes in its frequency components can therefore be used for the identification of the occurrence of a particular fault.

As described in section 2.5, although vibration and acoustics share similar generation mechanisms, their signal characteristics differ. In this study, the residual signals from the ICAN were used for a subsequent spectral analysis, because separation of residual signals provided by the ICAN allows easier interpretation than the single residual signal produced by the JCAN.

Figure 2 compares the spectra of the measured data from the induction motor with those of the network residuals. Figures 2a and c show the spectra of vibration data and acoustic data respectively and Figs 2b and d show the corresponding residual spectra. The spectra of the raw signals show a gradual increase in the amplitude of the 100 Hz component. This particular change allows a unique distinction to be made of the phase imbalance faults from other possible faults (such as shaft misalignment and bearing damage [**14**, **22**]). In the corresponding residual spectra, amplitude changes at 100 Hz are also clear. The change of this component in the vibration residual spectrum is 32 per cent higher than in the raw spectrum for case 1 and in the acoustic residual spectrum it is 200 per cent higher than in the raw spectrum. By comparison with conventional spectra, the residual spectra therefore

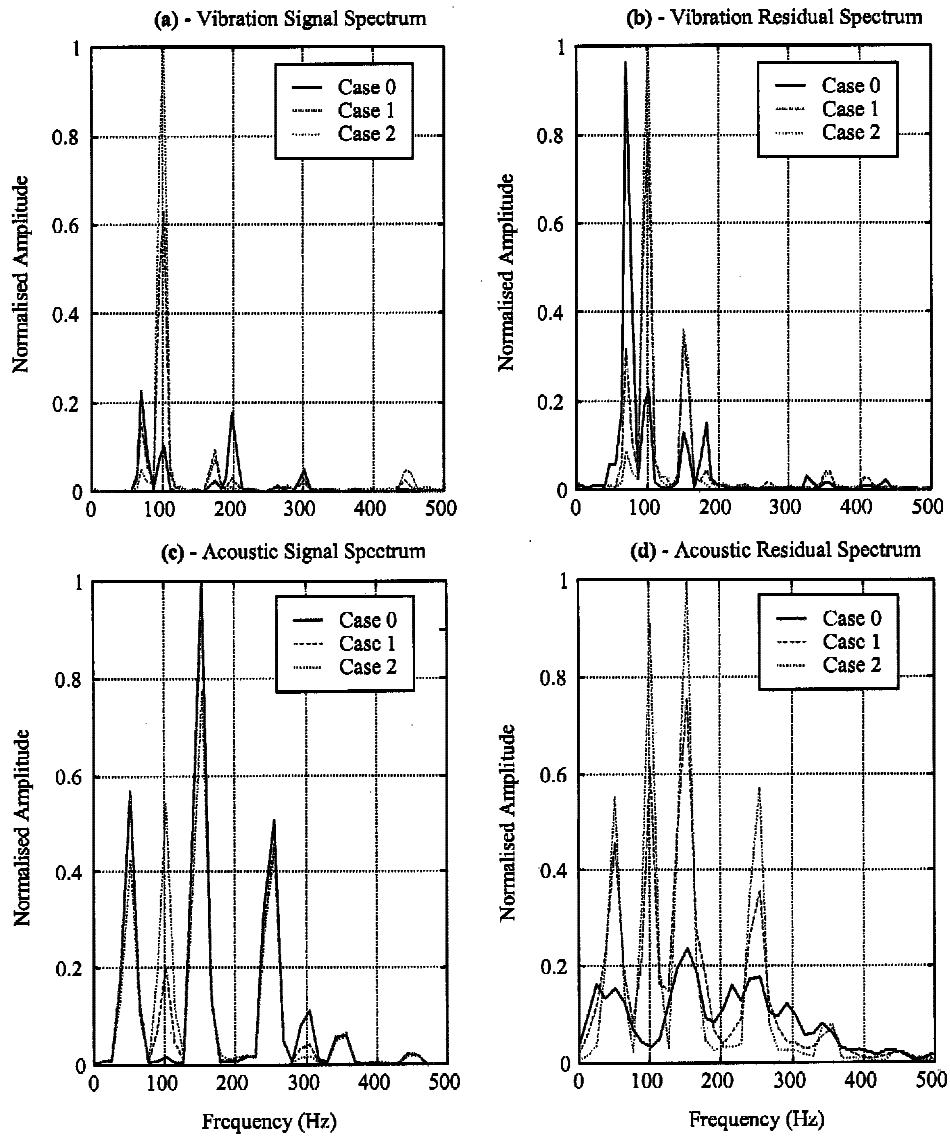

Fig. 2 Spectra of raw signals and residual signals from the ICAN

allow the characteristic fault feature (of the change in the 100 Hz frequency component) to be more clearly defined.

3 APPLICATION TO A NOVEL ELECTRIC MOTOR

3.1 Introduction

The second demonstration of componential coding is made through its application to flux data from a novel high-power electric motor prototype. This motor, a transverse flux motor, is currently being developed by Rolls-Royce plc and will potentially provide propulsion power for a range of future marine vessels.

From a theoretical perspective [**34**, **35**], changes of the magnetic flux profiles at different locations within the machine are likely to yield useful information on incipient fault conditions. Flux-based approaches to monitoring are currently being investigated for the transverse flux motor, and flux is routinely measured during operation. Although the effect of some failure modes on flux profiles may be predicted, the detection of particular profile changes is currently a labour-intensive process that requires visual examination and interpretation of individual waveforms. For a transverse flux motor in a working marine propulsion application this hands-on approach is not desirable. The application of componential coding to flux data from this machine therefore not only provides a demonstration of its ability to monitor novel machines, for which only limited information is available, but also provides automation of waveform analysis and basic level diagnosis (by separation of the types of profile changes from a healthy baseline case).

3.2 The transverse flux motor

Several features distinguish the transverse flux motor from other more conventional permanent magnet synchronous machines [**36**]:

1. The overall flux path is three-dimensional.
2. The stationary armature coils are simple solenoids.
3. The phases are entirely separated, with no electromagnetic coupling, providing fault tolerance and reversionary modes.
4. Substantial freedom of design is achieved by the ability to change the magnetic flux geometry and coil section.
5. The magnetic circuit does not interfere with the electric circuit.

The simplest transverse flux motor configuration (Fig. 3a) consists of a single rotor disc to which two opposite rotor rims are attached. The active rotor (Fig. 3b) comprises alternate soft iron laminated pole pieces and permanent magnets. The magnetization of the magnets is in the circumferential direction and aligned so that the pole pieces form alternate north (N) and south (S) poles. The stator consists of a number of C-shaped stator cores and a preformed coil that passes within them. The overall output shaft torque is achieved by the combination of the flux produced by the permanent magnets and that produced by the current in the solenoid.

3.3 Magnetic flux monitoring

Magnetic flux is an important operational characteristic in any electric machine. Unlike conventional electric motors, where physical access and design characteristics make flux monitoring difficult [**2**, **3**], the transverse flux motor is well suited to the monitoring of this parameter. In practice, this is achieved by placement of copper search coils around the machine. The induced voltage in these coils is directly proportional to the normal rate of change of flux density through the iron. The two main groupings of coil are those wound around the C-shaped stator cores and those embedded in the rotor at the interface between adjacent magnets and pole pieces. Those on the stator cores are located as illustrated in Fig. 4.

Previous work [**35**] has proven that visual analysis of the flux waveforms from the transverse flux motor in the time domain is particularly useful for detecting changes that can be directly attributable to machine characteristics. For example, manufacturing tolerances have previously been examined by an analysis of the phase relationship between waveforms [**35**], incipient sensor failures identified and a partial rotor demagnetization fault detected, diagnosed and located [**35**]. During the machine development stages only a small amount of flux data has been recorded and it has therefore been possible to analyse each waveform individually by eye and, consequently, make interpretations. However, two main problems exist in this approach. The first is in the detection of very small waveform changes from a data channel (that may only occur over a very small portion of the data covering one shaft revolution). The second problem is in performing this (presently visual) waveform inspection for a motor in service, where measurement of data will be continuous. These problems are compounded by the fact there are multiple sensors, all of which require examination ideally in a synchronous manner. The work described in this section illustrates how componential coding is able to address these problems.

3.4 Monitored magnetic flux data

To illustrate the potential of componential coding in application to the novel motor, six cases were defined

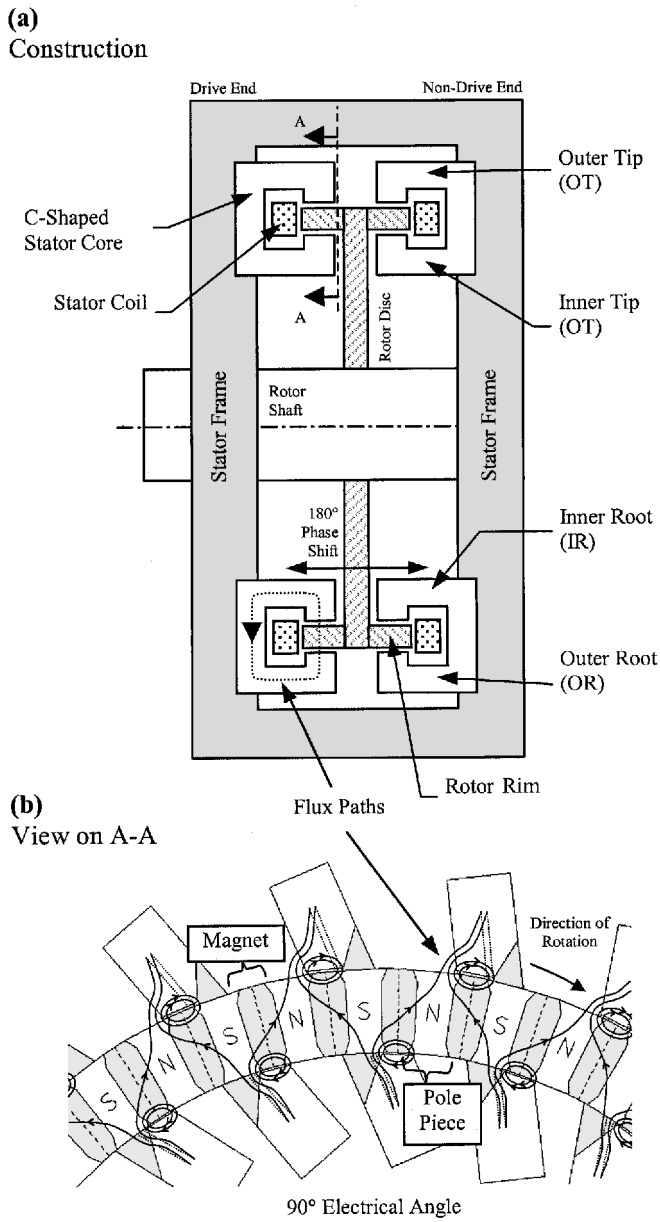

Fig. 3 Transverse flux motor configuration and flux paths

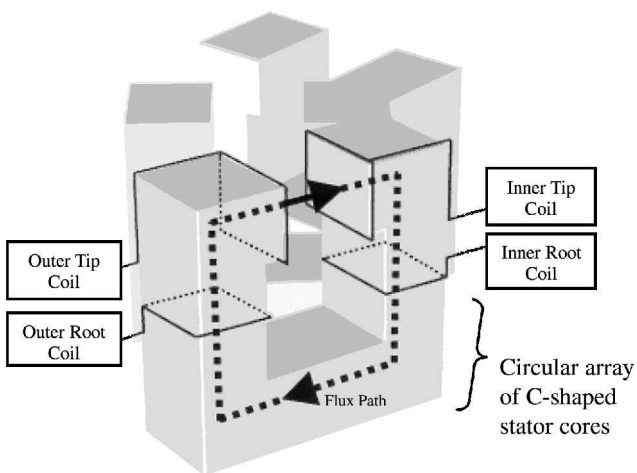

Fig. 4 Search coil positions on the stator core

based upon the type of search coil location from which data were collected and upon the date of acquisition (see Table 3, which defines cases 0 to 5). Separation was made on this basis because:

1. Different (stator) search coil locations are likely to yield slightly different flux profiles as a result of leakage flux path effects [**34**].
2. A stator component failure was experienced (and subsequently repaired) between the two acquisition dates (and it was possible some machine characteristics could have permanently changed).

Based on the available data, each case consisted of four channels of data recorded from four similarly located search coils.

Table 3 Outline of separated data cases

	Cases					
	0	1	2	3	4	5
Location type	Inner tip	Outer tip	Inner root	Inner tip and inner root	Outer tip	Rotor
Collection date	March 2000			August 2000		

Figure 5 provides an example segment from one of the four channels in each case. Initial visual examination of the data-sets revealed that three separate anomalous conditions were contained within them with respect to the data provided by all channels in cases 0 and 1 (the baseline profile expected from theory [**34**]). The baseline profiles have 38 uniform periods for each complete shaft revolution. This corresponds to the passing of 38 pole piece pairs on the rotor of this prototype. The first anomalous condition (channel 3 in case 2 and channel 1 in case 3) represents small and localized anomalies. The second anomalous condition (given by channel 1 in case 4) relates to severe distortion of most of the flux waveform. All channels in case 5 represent a third anomalous condition. Each of these channels provides flux information from the rotor (rather than stator). Therefore (as expected by theory [**34**]), the profiles are very different from the baseline flux for the stator search coils. As this difference is across the complete profile this is referred to as a global change compared with the baseline. Componential coding was applied to investigate its ability to detect and assess the severity of the three anomalous conditions described (particularly those small changes provided in cases 2 and 3).

3.5 Network training and optimization

Both the JCAN and ICAN were studied for their separation of the anomalies with respect to the baseline condition. The JCAN was employed to produce an overall anomaly detection result for each case (based on the four channels within each case and the phase relationships between them). Once the output from the JCAN provided an indication of change from the baseline, the ICAN was used to identify the anomalous individual data signals and identify/extract the anomaly features.

The dimension of basis vectors was set to 64 data points, as for the application to the induction motor data. For the basis vectors to cover two periods of the principal frequency component, the raw data were desampled. This was achieved using a Fourier transform-based approach, where a forward Fourier transform was implemented on data covering one complete revolution of the rotor (i.e. 38 periods) and an inverse Fourier transform was then applied to the first 1216 (i.e. 32×38) data points in the frequency domain. Desampling in this way was more suitable than the approach taken for the vibration and acoustic data because the flux data have little noise and are strongly periodic.

As with the application to induction motor data, both the threshold and the number of basis vectors were optimized using a genetic algorithm. Optimization was achieved by obtaining maximum discrimination (based on the ADI) between cases 0 and 1. The resulting configurations for the JCAN and ICAN are summarized in Table 4. Both the JCAN and ICAN have high values for the threshold. (For data vectors normalized to unit Euclidean norm, the theoretical maximum for useful threshold values is 1.) As discussed in section 2.4, this indicates that there is a strong similarity between input

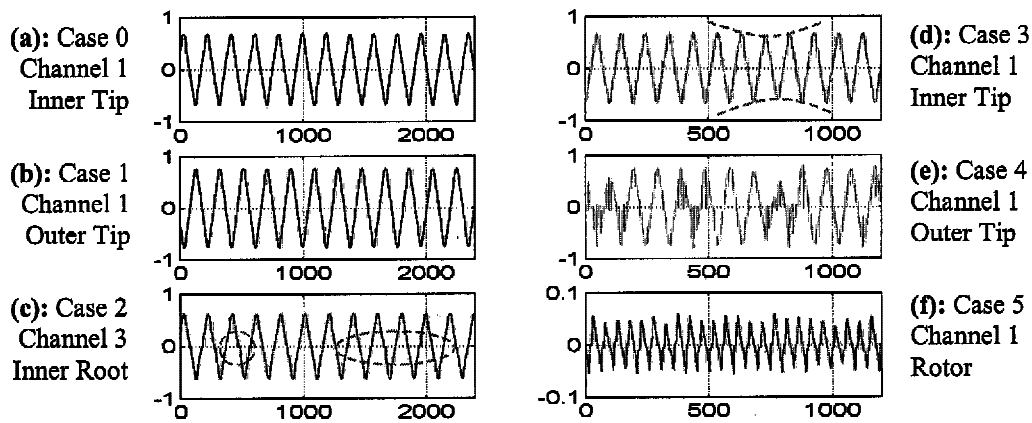

Fig. 5 Example segments of normalized flux data from different search coil locations

Table 4 Optimized componential coding configuration for transverse flux motor flux data

Componential coding variant Data-set	ICAN Channel 1, case 0	JCAN All channels, case 0
Basis vector dimension	64	256 (i.e. 64 + 64 + 64 + 64)
Threshold value	0.885	0.797
Number of basis vectors	4	5
ADI (case 0)	0.29	0.053
ADI (case 1)	0.807	1.022

patterns from the individual data-sets (whereas in the induction motor study, differences in the acoustic and vibration data-sets led to differences in optimized threshold values).

The optimized number of basis vectors for the ICAN and JCAN is much smaller than that in the induction motor study. The reason for this is that the flux data structures are much simpler in comparison to either the acoustic or vibration data.

3.6 Anomaly detection

Figure 6 illustrates the anomaly detection results obtained by the JCAN variant of componential coding. It produces an overall value of the ADI and VDI for each case presented to it. As the network is trained with respect to case 0, the reconstruction of newly monitored and previously unseen data, also from case 0, is very good. Hence the reconstruction error is small (close to 0) and so are the ADI and VDI values for this case.

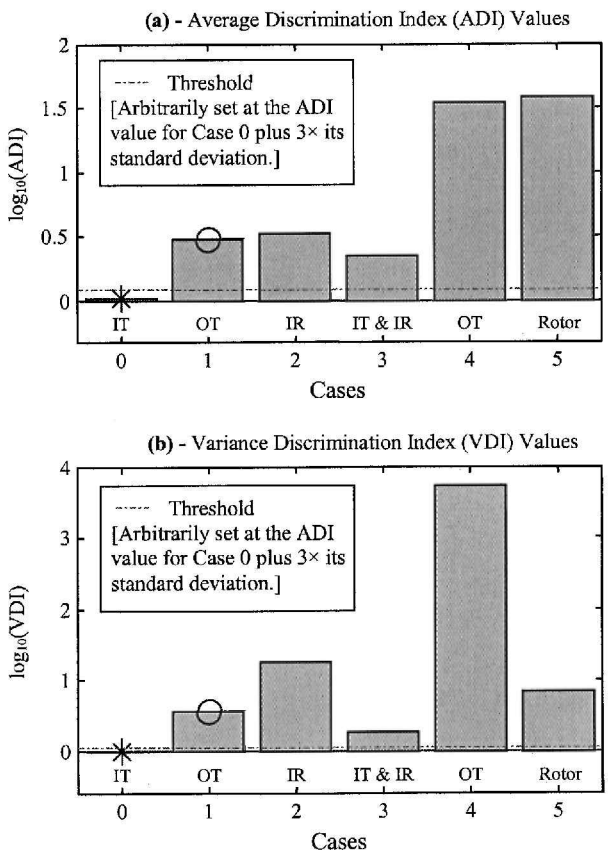

Fig. 6 Discrimination indices from the JCAN (✳ represents the training case, ○ represents the optimization case)

For those cases (1, 2 and 3) that have small visual differences from the baseline set (see Fig. 5), their ADI and VDI values are greater than the thresholds. The relatively small ADI and VDI values for case 3 relate to the fact that two of the four channels contained within it were very similar to the baseline case 0. The higher ADI value for case 2 reflects the waveform anomaly of channel 3 and the high value of the VDI highlights the fact that the anomaly occurs locally.

For case 1, although no anomalous features were observed in the raw data (Fig. 5b), relatively high values of the ADI and VDI were obtained. There are two possible reasons for this: differences in waveform profiles or phase differences between channels. The ICAN can be used to distinguish between these two hypotheses because the ICAN captures the statistics of individual channels. However, unlike the JCAN it is not capable of measuring phase relationships.

For cases 4 and 5, where there is a large variation from the baseline, the ADI values are much higher compared with those for the other cases with smaller variations. The VDI value for case 4 is higher than that for case 5. Because of the different ways the ADI and VDI interpret the reconstruction error, this implies that cases 4 and 5 contain local and global anomalies respectively. (The formulations of both the ADI and VDI are discussed in section 2.7 of Part 1 [**23**].)

The discrimination index values from componential coding allow separation of the five cases from the baseline one (case 0), discrimination between small and large differences and identification of local and global variations.

3.7 Anomaly diagnosis

The diagnosis of globally occurring anomalies can be achieved through residual spectrum analysis (demonstrated in section 2.6). However, residual spectra are not capable of identifying the locally occurring anomalies existing in transverse flux motor flux data. This is because the Fourier transform is inadequate at resolving

waveform changes that are small in amplitude, localized and positioned randomly. To overcome this problem, both ADI and VDI values can be used for the diagnosis of the small local anomalies.

Having detected the anomalies in each case by the JCAN, the ICAN was used to identify automatically the individual channels that cause these anomalies. Figure 7 presents the VDI values produced by the ICAN, as the VDI is more sensitive to the local small anomalies (see section 2.7 of Part 1 [**23**]). Based upon the difference in amplitude from the values in case 0, the VDI clearly captures nine anomalous channels (as indicated by * in Fig. 7). Seven of these were initially found by visual inspection of the raw data.

Two new anomalies (channel 3 of case 3 and channel 4 of case 4) were revealed by the high amplitudes of the VDI. These were not captured by the initial visual inspection procedure because they are very small waveform changes, occurring locally, and only once every shaft rotor revolution.

A better understanding of the localized anomalies can be achieved by calculation of individual ADI values for each input data pattern and plotting them against the angular position of the rotor. The obtained ADI is thus referred to as an instantaneous ADI. Figure 8 shows the ADI variation over two complete shaft revolutions. The localized changes in waveform produce large jumps in the ADI (well above the detection threshold, which was set at the ADI for case 0 plus three times its standard deviation). These high jumps not only allow the detection of the anomalies but also identify the angular position at which they occur. The characteristics of the ADI jumps also enable the identification of the mechanism causing the anomalies. For example, a single jump per revolution with a constant angular position (as in case 3) indicates a possible fault in one of the permanent magnets in the rotor. Several jumps per revolution spaced at a random angular position (as in cases 2 and 4) indicate a potentially faulty flux search coil.

By definition, the localized waveform changes cannot be measured accurately by the ADI and therefore the VDI was also used (see section 2.7 of Part 1 [**23**]). The combination of ADI and VDI produces comprehensive detection and diagnosis for both globally and locally occurring anomalies. This is illustrated in the scatter plot of these two indices. As shown in Fig. 9, those flux channels with *local* anomalies have a larger VDI than ADI. However, *global* changes (as in case 5) lead to similarly large amplitudes in both the VDI and ADI. Thus, local changes in a waveform can easily be distinguished from global ones, providing useful information in identifying the cause of the anomalies.

3.8 Benchmarking the capability of componential coding in condition monitoring

To benchmark the performance of machine monitoring using componential coding, its anomaly detection capability was compared with several established techniques currently in use. These techniques were: waveform measures (including root-mean-square and kurtosis), spectrum difference, cepstrum difference,

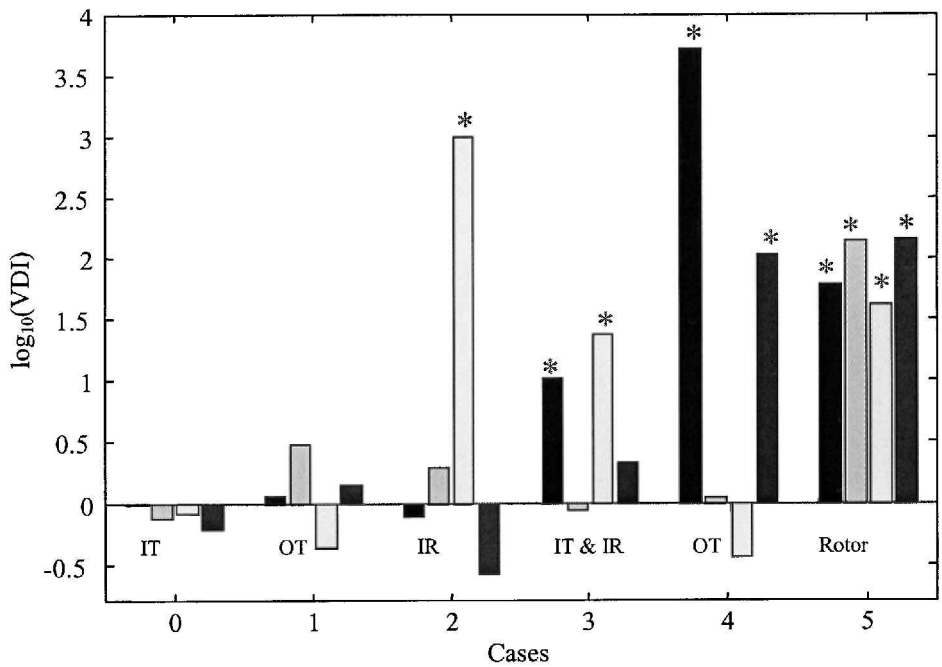

Fig. 7 VDI from ICAN channels and cases

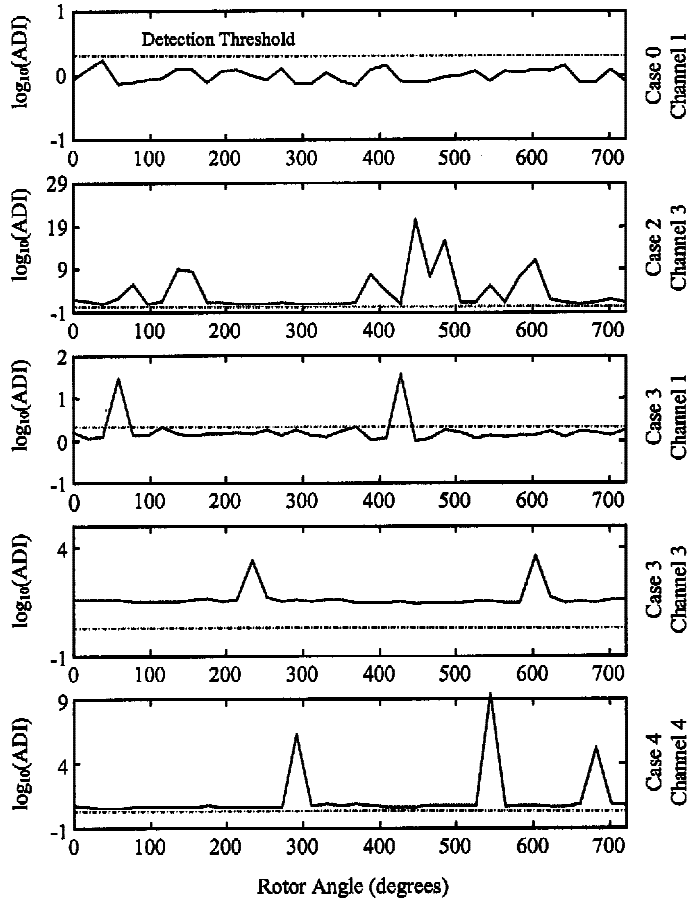

Fig. 8 Instantaneous ADI

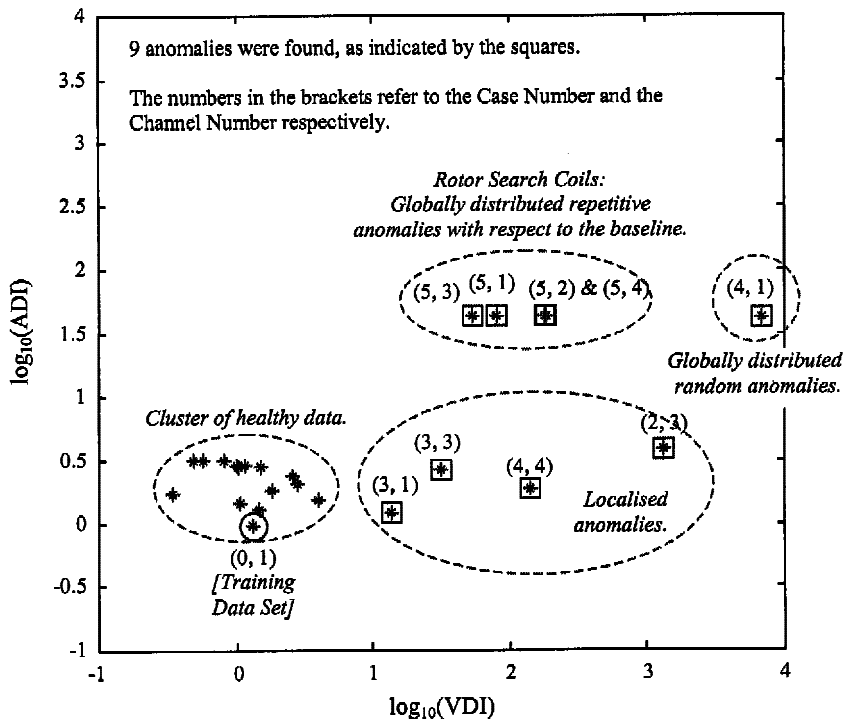

Fig. 9 Scatter plot of the ADI against the VDI

Fourier-based signal reconstruction and principal component analysis. Where possible, these techniques were optimized so that each of the anomalies could be most clearly separated from the baseline healthy data-set (case 0). For example, in the Fourier-based signal reconstruction method the number of Fourier components was optimized. The calculation of the waveform root-mean-square and kurtosis used the same size of input pattern (basis vector dimension) as componential coding. The calculation of the spectrum and cepstrum used longer input sizes to achieve better resolution. The Fourier-based reconstruction method and principal component analysis were used in a similar way to componential coding, in that a model was initially developed based on baseline data and then this was used to examine its ability to reconstruct the other cases. Following a genetic optimization (using a similar approach to that used for componential coding), the number of components for the Fourier-based reconstruction and the number of eigenvectors for principal component analysis was set to five and four respectively.

Table 5 shows the number of individual channels that could be separated as containing anomalies with respect to the baseline data. Componential coding enables all nine anomalous channels to be separated, but the very small and localized anomalies could not be detected by any of the conventional techniques. This demonstrates that, compared with the other methods assessed, monitoring using componential coding is the most comprehensive approach to detection of machine faults using motor flux search coil data.

4 SUMMARY AND CONCLUSIONS

Advanced data processing has the potential to enable earlier anomaly detection and more accurate diagnosis for electrical machine faults. This paper has presented the use of a novel unsupervised adaptive neural network, componential coding, for the condition monitoring of a conventional motor and a novel transverse flux motor. Componential coding is implemented by modelling characteristic baseline data and then using the model for automatic monitoring. The results show that the use of the single-valued average discrimination index (ADI) and variance discrimination index (VDI) provides a straightforward basis on which faults may be automatically detected and diagnosed.

Componential coding may be implemented through either of two network derivatives (JCAN or ICAN). To combine information from multiple sensor channels (yielding similar data structures) and perform speed critical on-line monitoring, the JCAN is the most efficient. However, it has been shown that the ICAN may be employed when either the information content from sensor channels is different (as in the application to induction motor vibration and acoustic data) or channel-level anomaly detection is required (as in the application to magnetic flux data).

Two approaches have been outlined for diagnosing the nature of anomalies. In can be concluded that the residual spectrum approach enables the classification of globally distributed changes. For example, voltage imbalance in the induction motor three-phase power supply was identified by the change in the 100 Hz component in the residual spectra. For small anomalies that occur over short segments of the data-sets (as experienced in the transverse flux motor flux data), the combination of the ADI and VDI enabled reliable classification. Furthermore, the application of an instantaneous ADI allowed identification of the position of the fault features.

A benchmark of componential coding against other conventional techniques (including waveform statistical measures, Fourier analysis and principal component analysis) has also been outlined in this paper. It can be concluded that, when applied to motor flux data, componential coding outperforms these techniques in that it can separate small, infrequently occurring and locally distributed anomalies not achievable to the same extent by the other approaches examined.

ACKNOWLEDGEMENTS

This work was carried out as part of Technology Group 10 of the MoD Corporate Research Programme. The Componential Coding algorithm is patented intellectual property of QinetiQ. Rolls-Royce plc is thanked for its support in application of this novel network architecture to electrical machines.

Table 5 Summary of comparisons of different detection performances

Technique	Anomalous channels detected	Detection performance (%)
Componential coding (ICAN implementation)	9	100
Fourier-based reconstruction	7	78
Principal component analysis	7	78
Waveform statistics	5	56
Spectrum difference	6	67
Cepstrum difference	7	78

© QinetiQ limited 2003. Published under licence with the permission of QinetiQ.

REFERENCES

1 **Starr, A.** and **Wynne, R.** A review of condition based maintenance for electrical machines. In *Handbook of Condition Monitoring*, 1996 (Elsevier Science, Oxford).

2 **Tavner, P. J.** and **Penman, J.** *Condition Monitoring of Electrical Machines*, 1987 (Research Studies Press, Baldock, Hertfordshire).

3 **Dorrel, D. G., Thomson, W. T.** and **Roach, S.** Analysis of airgap flux, current, and vibration signals as a function of the combination of static and dynamic airgap eccentricity in 3-phase induction motors. *IEEE Trans. Ind. Applic.*, 1997, **33**(1), 24–34.

4 **Seker, S.** Determination of air-gap eccentricity in electric motors using coherence analysis. *IEEE Power Engng Rev.*, 2000, **20**(7), 48–50.

5 **Wowk, V.** *Machinery Vibration—Measurement and Analysis*, 1991 (McGraw-Hill, New York).

6 **Finely, W. R., Hodowanec, M. M.** and **Holter, W. G.** An analytical approach to solving motor vibration problems. *IEEE Trans. Ind. Applic.*, 2000, **36**(5), 1467–1480.

7 **Eisenmann, R. C.** and **Eisenmann Jr, R. C.** *Machinery Malfunction—Diagnosis and Correction*, 2000 (Prentice-Hall, Englewood Cliffs, New Jersey).

8 **Hargis, P. K., Mahrt, R.** and **Doon, H. H.** The detection of rotor defects in induction motors. In Proceedings of IEEE International Conference on *Electrical Machines, Design and Applications*, 1982, pp. 216–220.

9 **Arthur, N.** and **Penman, J.** Induction machine condition monitoring with higher order spectra. *IEEE Trans. Ind. Electron*, 2000, **47**(5), 1031–1041.

10 **Thomson W. T., Rankin, D.** and **Dorrell, D. G.** On-line current monitoring to diagnose airgap eccentricity in large three-phase induction motors—industrial case histories verify the predictions. *IEEE Trans. Energy Conversion*, 1999, **14**(4), 1372–1378.

11 **Walliser, R. F.** and **Landy, C. F.** Determination of interbar current effects in the detection of broken rotor bars in squirrel cage induction motors. *IEEE Trans. Energy Conversion*, 1994, **9**(1), 152–158.

12 **Rankin, D. R.** The industrial application of phase current analysis to detect rotor winding faults in squirrel cage induction motors. *Power Engng J.*, 1995, **9**(2), 77–84.

13 **Liang, B., Payne, B. S.** and **Ball, A. D.** Detection and diagnosis of faults in induction motors using vibration and phase current analysis. In Proceedings of 1st International Conference on *The Integration of Dynamics, Monitoring and Control*, 2000, pp. 337–341.

14 **Payne, B. S., Ball, A. D., Gu, F.** and **Li, W.** A head-to-head assessment of the relative fault detection and diagnosis capabilities of conventional vibration and airborne acoustic monitoring. In Proceedings of the 13th International Congress on *Condition Monitoring and Diagnostic Engineering Management*, Houston, Texas, 2000, pp. 233–242.

15 **Schoen, R. R., Habetler, T. G., Kamran, F.** and **Barthheld, R. G.** Motor bearing damage detection using stator current monitoring. *IEEE Trans. Ind. Applic.*, 1995, **31**(6), 1274–1279.

16 **Eren, L.** and **Devaney, M. J.** Motor bearing damage detection via wavelet analysis of the starting current transient. *IEEE Instrum. Measmt Mag.*, 2001, **3**, 1797–1800.

17 **Gaylard, A., Meyer, A.** and **Landy, C.** Acoustic evaluation of faults in electrical machines. In IEE Proceedings of 7th International Conference on *Electrical Machines and Drives*, Durham, 1995, No. 412, pp. 147–150.

18 **Shibata, K., Takabashi, A.** and **Shirai, T.** Fault diagnosis of rotating machinery through visualisation of sound signals. *Mech. Systems and Signal Processing*, 2000, **14**(2), 229–241.

19 **Albright, D. R.** Method and apparatus for detecting rotor flux variations in the air-gap of a dynamo-electric machine. United States Patent Office, US Pat. 3506914, Patented April 1970.

20 **Penman, J., Dye, M. N., Tait, A. J.** and **Bryan, W. E.** Condition monitoring of electrical drives. *Proc. IEE, Part B*, 1986, **133**(3), 142–148.

21 **Payne, B. S., Ball, A. D.** and **Gu, F.** Detection and diagnosis of induction motor faults using statistical measures. *Int. J. Condition Monitoring and Diagnostic Engng Managmt*, 2002, **5**(2), 5–19.

22 **Lyon, R. H.** *Machinery Noise and Diagnosis*, 1987 (Butterworth Publishers, London).

23 **Webber, C. J. S., Payne, B. S., Gu, F.** and **Ball, A. D.** Componential coding in the condition monitoring of electrical machines. Part 1: principles and illustrations using simulated typical faults. *Proc. Instn Mech. Engrs, Part C: J. Mechanical Engineering Science*, 2003, **217**(C8), 883–899.

24 **Chow, M.** and **Yee, S.O.** Application of neural networks to incipient fault detection in induction motors. *J. Neural Network Computing*, 1991, **2**(3), 26–32.

25 **Filippetti, F.** Neural networks aided on-line diagnostics of induction motor rotor faults. *IEEE Trans. Ind. Applic.*, 1995, **31**(4), 892–898.

26 **Paya, B. A., Esat, I. I.** and **Badi, M. N. M.** Artificial neural network based fault diagnosis of rotating machinery using wavelet transforms as a pre-processor. *Mech. Systems and Signal Processing*, 1997, **11**(5), 751–765.

27 **Luo, F.** and **Unbehauen, R.** *Applied Neural Networks for Signal Processing*, 1997 (Cambridge University Press, Cambridge).

28 **Bonnett, A. H.** and **Soukup, G. C.** Cause and analysis of stator and rotor failures in three-phase squirrel-cage induction motors. *IEEE Trans. Ind. Applic.*, 1992, **28**(4), 921–937.

29 **Arkan, M., Perovic, D. K.** and **Unsworth, P.** Online stator fault diagnosis in induction motors. *Proc. Electl Power Applic.*, 2001, **148**(6), 537–547.

30 **Pierrat, L.** and **Morrison, R. E.** Probabilistic modelling of voltage asymmetry. *IEEE Trans. Power Delivery*, 1995, **10**(3), 1614–1620.

31 **Ball, A. D, Li, W., Gu, F.** and **Shi, Z.** The analysis of engine acoustic signals using higher order statistics. In Proceedings of 4th Annual Maintenance and Reliability Conference, Knoxville, Tennessee, 2000, Vol. 2, pp. 33.01–33.09.

32 **Gu, F., Payne, B. S.** and **Ball, A. D.** Optimisation of a self-organising autoencoder for the condition monitoring of a

novel electric motor. University of Manchester Document MERG-0600, 2000.

33 **Elhaj, M., Gu, F., Shi, Z.** and **Ball, A. D.** A comparison of the condition monitoring of reciprocating compressor valves using vibration, acoustic, temperature and pressure measurements. In Electronic Proceedings of 6th Maintenance and Reliability Conference, Knoxville, Tennessee, 2002.

34 **Payne, B. S., Voyce, J., Husband, M.** and **Ball, A. D.** Development of condition monitoring technology for electric propulsion systems. In IMarEST Proceedings of International Naval Engineering Conference, Bath, 2002, pp. 238–247.

35 **Payne, B. S., Husband, M., Simmers, B., Gu, F.** and **Ball, A. D.** The development of flux monitoring for a novel motor. In Proceedings of the 14th International Congress on *Condition Monitoring and Diagnostic Engineering Management*, Manchester, 2001, pp. 353–360.

36 **Mitcham, A. J.** Transverse flux motors for electric propulsion of ships. In IEE Colloquium, 1997, pp. 3/1–3/6.